A Simple Method for Designing Infiltration Low Impact Development Techniques Considering Effects of Urbanization and Climate Change

Marcus Nóbrega Gomes Jr.[a], Cesar A. F. do Lago[b], Eduardo Mario Mendiondo[b]

[a] *University of Arizona, Department of Hydrology and Atmospheric Sciences, James E. Rogers Way, 316A, Tucson, 85719, Arizona, United States of America*
[b] *University of Sao Paulo - Av. Trab. Sao Carlense 400 - Parque Arnold Schimidt Sao Carlos - SP 13566-590 Brazil*

Abstract

Infiltration low-impact development (LID) techniques allow the slow infiltration of surface water, reducing peak volumes and flows. Their design consists of specifying the surface area and a maximum ponding depth to guarantee the minimum volume required to combat the effect of excessive urbanization. Arbitrary specifications of the design height (i.e., the maximum ponding depth) of these LIDs can lead to undersizing of the minimum area required. In this paper, an optimized design model for retention catchments (MoDOBR) is developed, implemented, and tested under four examples. We hypothesize that is necessary to match the maximum ponding depth with the depth required to store excess runoff in case the media and the underdrains are clogged. The model solves mass balances on the surface of the LID and at the interface of the saturated soil layer. The results of four numerical examples are presented, and the influence of different soil types is discussed through sensitivity analyses. Overall results indicate that if the LID is designed in sandy soil, it requires a surface area of 2.9% of the catchment, while if it is designed in clayey soil, the required area would be 50% of the catchment area for a 5-year rainfall design storm.

Keywords: Design of Retention Ponds, Pre-development, Optimization of Retention Ponds, Low Impact Development

1. Introduction

Retention basins are LIDs that aim to temporarily store surface runoff to slowly provide flow discharge to local drainage systems and an increase in the proportion of surface runoff becoming subsurface recharge (i.e., increase volume reduction) (Baptista et al., 2011; Fletcher et al., 2015). Techniques that favor infiltration of surface runoff, such as retention reservoirs, can attenuate both flows and peak times (Winston et al., 2016). In areas where the soil has relatively good infiltration capacity, retention reservoirs are solutions that can be both economically and technically viable (Mano et al., 2008), in addition to contributing to the restoration of the pre-urbanization flow regime.

Some mathematical models can be used to simulate the hydrological behavior of retention basins. In general, models that solve water balances are suitable for evaluating the runoff of retention basins. The PULS (Zoppou, 1999) is one of the most widely used methods for sizing retention basins. The PULS method consists of solving the mass balance taking into account precipitation, inflow and percolation. By its simplicity, PULS method can be easily solved in numerical spreadsheets (Júnior, 2019; Gomes Jr et al., 2023; Ferreira et al., 2019). From a maximum outflow determined for the project, it is possible to calculate the minimum volume of the retention basin. Other alternative is the Stormwater Management Model (SWMM) software which contains a module for analyzing low-impact LIDs where it is possible to parameterize bioretention or rain gardens (Rossman and Huber, 2016). Fundamental mass and energy balance equations are applied in SWMM to determine the inlet and outlet hydrographs of these systems. Another example is the DRAINMOD software, which works on a daily time scale (Skaggs et al., 2012) but has recently been adjusted to handle faster flows on a sub-daily time scale (Braswell et al., 2024).

Retention basin designs must specify the reservoir surface area, the maximum ponding depth, and, eventually, the size of the overflow devices, if necessary. These, in many cases, are designed for return periods greater than those of typical low-impact drainage design conditions, in some cases for return periods of up to 200 years (Fletcher et al., 2015).

One of the most applicable methods for the design of LIDs is the zero-impact criterion (PG County, 2007). This method considers two scenarios: the pre-urbanization scenario, where the drainage area likely had more natural land use and less urbanization, and the post-urbanization scenario, where previously permeable areas become urbanized, favoring the generation of surface runoff. A significant difference in runoff generation occurs when comparing the volumes of effective precipitation generated by each scenario. Based on the volumetric difference of both methods, the minimum storage volume is determined, and based on the pre-urbanization peak flow, spillways are designed to reduce effluent flows to the pre-urbanization flow (Rosa, 2016).

Another method applicable to LIDs is the envelope curve method (Santos et al., 2021; Silveira and Goldenfum, 2007). The method considers a constant outflow flow rate over time. It assumes an inlet hydrograph such that the inflow rate is proportional to the precipitation intensities from the Intensity-Duration-Frequency (IDF) curve, and infiltration from the upstream catchment is modeled with the rational method. By calculating the accumulated volumes of effective precipitation and the outflow flow rate, the maximum difference between both volumes is determined, similarly to the Rippl method (Tomaz, 2003).

Both the envelope curve and the zero-impact method follow the same hydrological principle of attempting to reduce the impacts of urbanization through the use of LIDs that provide volumetric storage of surface runoff generated by excessive urbanization. Although both methods serve as a basis for the pre-design of retention basins, neither of them considers the temporally variable hydrological behavior of compensatory infiltration techniques, which have non-linear behavior (Gomes Jr et al., 2023; Júnior, 2019). Duke et al. (2024) showed that even the lack of a dynamic record of the water level in LIDs within independent rainfall events could compromise their mitigation capacity, showcasing the temporal hydrological performance of these systems and the role of proper initial conditions for the simulations.

As opposed to dynamic models, explicit simplified methods such as the Envelope Curve are an option for pre-design (Silveira and Goldenfum, 2007). Although the envelope curve method is an alternative for design retention basins, since it considers the outflow flow rate constant over time, the method disregards the temporal variability of the infiltration process. On the other hand, the Richards equation (Richards, 1931), the most widely accepted model for simulating vadose processes and hence infiltration modeling, is too complex to be widely applied in pre-design applications done manually or in simple spreadsheets. Furthermore, explicit solutions in time of the Richards partial differential equation with good numerical stability for application in simple spreadsheets are too complex given the discretization methods required for its solution. Alternatively, the physically-based model of Green-Ampt (Green and Ampt, 1911), which can be derived from simplifications in the Richards equation, can capture the nonlinear behavior of infiltration and has the advantage of being relatively easy to implement (Gomes Jr et al., 2023; Júnior, 2019).

The objective of this work is to present a fast and efficient method for designing retention basins and other infiltration techniques considering the temporal variation of infiltration at the techinque surface. By obtaining the minimum depth necessary to guarantee the storage of the minimum volume to combat the effects of excess urbanization, the designs provided by the developed model allow also a scenario of fulll clogging of the media and its hydraulic devices. It is important to emphasize that the minimum storage volume of surface runoff does not necessarily coincide with the flooding volume modeled by the non-linear hydrological simulation, so the solution to the problem must be found by trial and error or by optimization algorithms.

Given the imminent impacts of climate change and the non-stationarity of the IDF curves (Paiva et al., 2024), this paper also proposes a flexible method that considers the design of the freeboard of the LID taking into account excess runoff generated by climate change. Four examples are solved. The first example presents a typical condition for designing a retention basin for a $5,000$ m^2 area for a given known design soil. The second example evaluates the effect of different soil types on calculating compatible heights. The third example evaluates a case where a bottom orifice is used as a flow-regulating device to ensure that an adopted height of 80 cm is feasible to make the volumes compatible. The last approach of this paper presents the sensitivity analysis of all parameters of the hydrological model for typical soil conditions.

2. Methods

2.1. Model for Optimized Design of Retention Basins (MoDOBR)

This section presents the mathematical approach for determining the inflow hydrograph and the dissipation of the inflow as infiltrated flow at the base of the reservoir. The conceptual model corresponds to a small catchment, modeled by the rational method, which discharges into a retention basin that slowly propagates the inflow to the water table .

The peak discharge of the rational method is given by (Mulvaney, 1851; Kuichling, 1889):

$$Q^p = C \cdot i \cdot A_c \tag{1}$$

where Q^p is the peak discharge of the triangular hydrograph of the rational method $[\mathrm{L} \cdot \mathrm{T}^{-3}]$, C is the average runoff coefficient of the contributing basin [-], i is the precipitation intensity $[\mathrm{L} \cdot \mathrm{T}^{-1}]$ and A_c is the drainage area $[\mathrm{L}^2]$. An assumption herein is made by neglecting the effect of the effect of the retention basin area into A_c. Therefore, A_c models only the contributing area to the retention basin.

The previous equation is valid for pre- and post-urbanization conditions, with the differences for each case adjusted by the runoff coefficients and time of concentrations. The design precipitation intensity is a function of the time of concentration which can be estimated by a variety of expressions (Silveira, 2005). One such formulation is the SCS-Lag equation, given by (NRCS, 2010):

$$t_c = 23.19\Big[\frac{l^{0.8}\,(S_{\mathrm{SCS}}+1)^{0.7}}{1140Y^{0.5}}\Big] \tag{2}$$

where t_c is given in minutes, l is the surface runoff length [m], Y is the average basin slope [%], S_{SCS} is the infiltration potential [mm] given by $25400/\mathrm{CN}-254$ and CN is the curve number of the NRSC-CN method.

Several formulations are available to determine the design intensity. In this paper, the Sherman-type curve is adopted and is written as (Gomes Jr et al., 2021):

$$i = \frac{K \cdot \mathrm{TR}^a}{(b+t_c)^c} \tag{3}$$

where K, a, b and c are the terms of the IDF curve and TR is the return period.

With the peak discharge and the time of concentration, it is possible to plot continuous functions that describe the rise and fall of the triangular hydrograph of the rational method. These expressions are written as:

$$\begin{aligned} Q(t) &= Q_p \cdot \Big(\frac{t}{t_c}\Big),\ \text{If } t \leq t_c \\ Q(t) &= Q_p \cdot \Big[\min\Big(\frac{t-t_c}{t_c}, 0\Big)\Big],\ \text{If } t > t_c, \end{aligned} \tag{4}$$

where $Q(t)$ is the instantaneous discharge of the triangular hydrograph of the rational method $[\mathrm{L}^3 \cdot \mathrm{T}^{-1}]$.

The difference between the pre- and post-urbanization volumes provides the minimum storage volume required for detention reservoirs. This volume is easily calculated by integrating the inlet and outlet hydrographs and calculating the difference between them, which is mathematically written as the maximum argument between the integral of both hydrographs:

$$V_{\min} = \underset{t\in\tau}{\operatorname{argmax}}\Big[\int_0^t \Big(Q_{\mathrm{pos}}(t) - Q_{\mathrm{pre}}(t)\Big)\mathrm{dt}\Big] \tag{5}$$

where the function argmax represents the maximum argument of the operand and τ represents the duration of the simulation.

The volume $V_{\min}$ is the minimum storage volume that a reservoir must support to guarantee the pre-urbanization volumetric conditions. In other words, it is the volume that a reservoir structure must have to compensate for the excess runoff generated by post-urbanization, compared to the pre-urbanization runoff generation conditions, if the filter medium is clogged and the drainage devices are not in operation. This hypothesis is particularly important when considering aging infrastructure and lack of maintenance that eventually would occur in such type of LID system.

Drainage devices can be coupled to the reservoir to favor the flow output either through orifices, weirs, or pumps (Gomes Jr et al., 2023; Gomes Júnior et al., 2022). In the particular case of infiltration basins, the main flow regulating device is the infiltration flow rate at the base of the reservoir. Since these are typically reservoirs where the surface dimensions are relatively larger than the height, lateral infiltration can be neglected. In the case of smaller techniques, such as rain gardens or permeable pavements, consideration of lateral infiltration is important (Gomes Jr et al., 2023; Lee et al., 2015). For parsimony, in the MoDOBR model, lateral infiltration is negligible, assuming that the reservoir has low heights relative to the surface dimensions.

In general, the infiltration capacity of the seepage soil can be estimated by the Green-Ampt method (Green and Ampt, 1911), which, taking into account the physical properties of the soil, estimates its infiltration capacity as:

$$C(t) = k_{\text{sat}} \frac{\Delta\theta \Big(\psi + h_p(t)\Big)}{F(t)} \tag{6}$$

where k is the saturated hydraulic conductivity of the soil, ψ is the suction pressure and h_p is the flooded height at the surface of the infiltration basin, F is the accumulated infiltration in the soil and $\Delta\theta$ is the effective porosity of the soil (Green and Ampt, 1911).

By considering relatively small time-steps, one can derive the seepage infiltration rate is given as a function of the infiltration capacity and the inflow rate, so that:

$$f(t) = \min\Big(C(t),\ h_p(t)/\Delta t\Big) \tag{7}$$

The previous equation approximates the non-linear infiltration Green-Ampt equation that typically has to be solved with gradient-based algorithms to a simple explicit equation that has hence to be solved in smaller time-steps.

The accumulated infiltration is determined by the integral of the infiltration capacity and is given by:

$$F(t + \Delta t) = F(t) + \Delta t \cdot f(t) \tag{8}$$

Similarly, by performing a mass balance on the surface of the reservoir, a dynamic equation of the ponding depth is obtained, given by:

$$h_p(t + \Delta t) = h_p(t) + \Delta t \cdot \Big(Q(t)/A - f(t) - S(t)\Big) \tag{9}$$

where $S(t)$ models inputs or outputs of the control volume (e.g., drainage by orifices, weirs, irrigation, evapotranspiration)

From the simulation results, the maximum ponding depth is defined as $h_p^{\max} = \max\limits_{t \in \tau}(h_p(t))$

2.2. Detention Time Restriction

An important criterion in the design of LIDs that receive rainwater and have a ponding depth is the detention time. Due to the proliferation of waterborne diseases, it is important that the duration of the ponding depth emptying does not exceed 24 h - 48 h. In this article, we adopt 24 h as the maximum ponding depth emptying time (t_d). Numerically, we seek to determine the time t_v that the ponding depth is less than or equal to a tolerance height δ (e.g., 1 mm).

	Detention Ponds				Retention Ponds										
	(Eq. 1)	(Eq. 1)	$(Q_{pos} - Q_{pre})\Delta t$	(Eq. 5)	(Eq. 8)	(Eq. 9)	h(t) x A / 1000	(Eq. 6)	(Q_{pos} / A)	Source Term	$h_p / \Delta t$	(Eq. 7)	f x A	(Eq. 8)	(Eq. 9)
t(min)	$Q_{pré}(t)$ [m^3/s]	$Q_{pós}(t)$ [m^3/s]	ΔV (m3)	V_{acum} (m^3)	F(t) [mm]	hp(t) [mm]	Vol [m^3]	C [mm/h]	Qin [mm/h]	S(t) [mm/h]	Pin [mm/h]	f [mm/h]	Qinf [m^3/s]	$F(t + \Delta t)$ [mm]	$h(t+\Delta t)$ [mm]
0	0.00	0.00	0.00	0.00	5.00	0.00	0.00	176.88	0.00	0.00	0.00	0.00	0.00	5.00	0.00
1	0.00	0.01	0.58	0.58	5.00	0.00	0.00	176.88	613.40	0.00	0.00	0.00	0.000	5.00	10.22
2	0.00	0.02	1.17	1.75	5.00	10.22	0.67	201.42	1226.80	52.65	613.40	201.42	0.004	8.36	26.44
3	0.00	0.03	1.75	3.51	8.36	26.44	1.72	155.84	1840.20	84.66	1586.14	155.84	0.003	10.95	53.10
4	0.01	0.04	2.34	5.85	10.95	53.10	3.46	155.21	2453.60	119.98	3185.84	155.21	0.003	13.54	89.40

Figure 1: Example of a spreadsheet script for sizing. The expressions used to calculate each column are shown in the figure, including the representative equations from this manuscript.

2.3. Coupling Design Heights

As aforementioned, a detention or retention reservoir design must specify at a minimum the storage surface area and height. For a given $V_{\min}$ and a given reservoir design height h, the reservoir surface area assuming a prismatic volume is:

$$A = \frac{V_{\min}}{h} \tag{10}$$

The area (A) calculated for the design height [L^2] is such that, in a case of total absence of infiltration (e.g., a case where the filter is clogged), the reservoir can store all the excess volume caused by urbanization above pre-urbanization conditions. In the design of infiltration basins, part of this stored volume is dissipated as bottom infiltration due to the infiltration capacity of the soil, which would eventually require a design height different from the one adopted.

The design problem proposed in this article, therefore, consists of determining a combination of infiltration basin area (A) and height (h) so that the volume $V_{\min}$ is met and that the maximum ponding depth $(h_p^{\max})$ is less than or equal to the design height and the emptying time is less than t_d.

More specifically, since the volume is determined by the pre- and post-urbanization conditions and the area of the retention basin is a function of this volume and the design height, the design consists of determining the height h that satisfies the height coupling and emptying time constraints. In this way, the minimum volume is simultaneously met to combat the volumetric effects of post-urbanization while ensuring a flooded height that does not cause overflows or is oversized, in addition to avoiding long emptying times that increase the chances of proliferation of waterborne vectors.

By restricting the height h to be exactly equal to the maximum ponding depth to ensure the smallest possible area, a design problem can be developed via an optimization problem, given by:

Coupled Design Height

$$\begin{aligned} \underset{h}{\text{minimize}} \quad & \left|(h - h_p^{\max})\right| \\ \text{subject to:} \quad & h_{\min} \leq h \leq h_{\max} \\ & \text{Eq. (5) to Eq. (10)} \\ & t_{\text{v}} \leq t_{\text{d}} \end{aligned} \tag{11}$$

where $h_{\min}$ and $h_{\max}$ are the minimum and maximum heights tolerable in the design (e.g., 0.1 m to 2-3 m, depending on the geotechnical conditions). In cases where there is no viable solution to the problem in Eq. (11), another LID technique should be employed.

The problem proposed in Eq. (11) guarantees not only the case where both areas are compatible but also the smallest possible retention basin surface area, ensuring more economically viable solutions. The MoDOBR model is implemented in a spreadsheet and the solution of the optimization problem mentioned above is done by the non-linear GRG method of the Excel solver (Smith and Lasdon, 1992). A spreadsheet script for performing the sizing is presented in Fig. 1.

2.4. Freeboard and Protective Structure to Combat Floods and Climate Change

Recent studies indicate that increases in precipitation in South America due to climate change may vary by 20 to 40% for a given return period (Paiva et al., 2024). The factor γ is defined as:

$$i_d(\mathrm{TR}, \mathrm{t_c}) = \gamma \cdot i(\mathrm{TR}, \mathrm{t_c}) \tag{12}$$

where i_d is the freeboard design precipitation taking into account climate change, γ represents the design precipitation upscaling factor used in the design, and i is the design precipitation using the most up-to-date IDF. For notational simplicity, $i_d(\mathrm{TR}, \mathrm{t_c}) = i_d$ and $i(\mathrm{TR}, \mathrm{t_c}) = i$.

The freeboard h_b is designed to counter the effect of the volumetric increase due to climate change for the design return period. Assuming the same time of concentration with and without climate change, calculating the volumetric difference of the post-urbanization and post-urbanization hydrographs with climate change, and isolating h_b, we obtain:

$$h_b = \frac{C_{\mathrm{pos}} \cdot \Big[(\gamma - 1) \cdot i(\mathrm{TR})\Big] \cdot A_c \cdot t_c}{A} \tag{13}$$

where the term $(\gamma - 1)$ represents the exclusive effect of climate change on the design precipitation.

In addition to the freeboard, an overflow structure must be designed to prevent overtopping from the sides of the retention basin. In this case, a longer return period (e.g., 10-25 years) is recommended. Using basic hydraulic equations, the surface spillway can be modeled with a Francis-type equation, which can be summarized in the following format (Porto, 2004):

$$Q^{p*} = C_d \cdot L_{\mathrm{ef}} \cdot (h + h_b - h_s)^{3/2}, \tag{14}$$

where C_d is approximately 1.8, L_{ef} is the effective length of the weir sill, h is the design height of the LID, h_s the spillway crest height taken from the surface of the retention basin (typically adopted as h) and $Q^{p*} = C_{\mathrm{pos}} \cdot i_d(\mathrm{TR}_v) \cdot A$ is the peak discharge calculated with the design intensity taking into account the increase due to climate change and the return period used for the weir calculation (TR_v).

By fixing the spillway crest height h_s and isolating L_{ef} in Eq. (14), an expression is obtained that calculates the effective spillway length that avoids overtopping for the design event, so that:

$$L_{\mathrm{ef}} = \frac{C_{\mathrm{pos}} \cdot i_d \cdot A}{C_d \cdot (h + h_b - h_s)^{3/2}} \tag{15}$$

It is possible to incorporate the dynamic equation of the weir into the mass balance of the LID (Eq. (9)) by replacing h with $h_p(t)$ in Eq. (14) and subsequently including a source term $S(t)$ that considers the weir flow. In this case, lower design heights would be designed because if $h_p(t)$ exceeds h_s, the weir flow would release flows, reducing the maximum flooded height dynamically. In this article, this effect is disregarded by the same previously used hypothesis that it could be clogged by waste throughout its useful life, and the maximum freeboard volume designed is such that it would be able to store the excess runoff due to loss of efficiency and climate changes without the need for overflow.

The input parameters for the problem are:

- Soil hydraulic conductivity (k_{sat})
- Soil suction head (ψ)
- Initial moisture condition of the infiltration soil ($F(0)$) from Eq. (8).
- Initial ponding depth ($h_p(0)$)
- Temporal discretization (Δt)
- Final simulation time (t_f)

- IDF curve parameters K, a, b and c
- Pre- and post-urbanization runoff coefficient
- Pre- and post-urbanization time of concentration.

3. Example 1 - Typical design condition

A commercial area in Sao Carlos - Sao Paulo with 5,000 m^2 of area with 40% of impervious areas ($C = 1$), 60% of permeable areas ($C = 0.6$) must receive an infiltration reservoir to contain the 5-year return period event. The time of concentration of the basin in the urbanized state is 10 minutes. In pre-urbanization conditions, the region was pastureland, with $C = 0.35$ and a time of concentration of 25 minutes. The parameters of the IDF curve are $K = 819.67$, $a = 0.138$, $b = 10.77$, $c = 0.75$ (Gomes Jr et al., 2021). The reservoir to be designed in predominantly sandy soil has infiltration parameters $k = 120.4\ \mathrm{mm} \cdot \mathrm{h}^{-1}$, $\Delta\theta = 0.42$, $\psi = 49.5$ mm and the initial design conditions are $F(0) = 5$ mm and $h(0) = 0$ mm.

Determine the area and height of the retention basin assuming that the maximum ponding depth is equal to the design ponding depth of the basin, solving Eq. (11) and compare the results with a case where the height is arbitrarily adopted as 0.8 m.

3.1. Solution

The post-urbanization runoff coefficient is given by the weighted average of the areas, being:

$$C_{\mathrm{pos}} = (0.4 \times 1 + 0.6 \times 0.6) = 0.76$$

Substituting the post-urbanization time of concentration in the IDF curve, we obtain:

$$i_{\mathrm{pos}} = \frac{819.67 \cdot \mathrm{TR}^{0.138}}{(10.77 + 10)^{0.75}} = \frac{819.67 \cdot 5^{0.138}}{(10.77 + 10)^{0.75}} = 69.68\ \mathrm{mm} \cdot \mathrm{h}^{-1}$$

The post-urbanization peak flow is therefore:

$$Q^{p}_{\mathrm{pos}} = C_{\mathrm{pos}} \times i_{\mathrm{pos}} \times A = 0.76 \times (69.68/1000/3600) \times 5000 = 0.111\ \mathrm{m}^3 \cdot \mathrm{s}^{-1}$$

Similarly, applying the previous equations, the pre-urbanization peak flow is determined

$$Q^{p}_{\mathrm{pre}} = 0.034\ \mathrm{m}^3 \cdot \mathrm{s}^{-1}$$

Performing the evolution of the hydrographs from Eq. (4), we obtain the pre and post urbanization hydrographs as illustrated in Fig. (2)(b). The storage volume V_{min} results in 52.14 m^3. Firstly, using the model already programmed, imagining a design height $h = 0.8$ m would result in an area of 65.18 m^2 and an area equal to 1.3% of the area of the contributing basin. The results of the hydrological simulation, without determining the optimal design height by Eq. (11), show an undersizing scenario. The maximum ponding depth is higher than the design height adopted for the reservoir.

In the case where the height is adopted arbitrarily, there is no guarantee that the ponding depth is less than or equal to the specified height. The results in Fig. 2 reveal a maximum ponding depth of 88 cm, higher than the maximum.

Solving Eq. (11), the result is a height of 0.36 m and an area of 2.9% of the contributing area (143 m^2). In this case, to ensure the storage of the volume V_{min} in a case of complete clogging of the retention basin, while avoiding overtopping, a lower height is required. This lower height ensures more surface area, which alters the infiltration flow regime so that the maximum volume stored due to the flooding generated by the excess runoff is equal to the chosen design height. The temporal evolution of the model states is shown in Fig. 2.

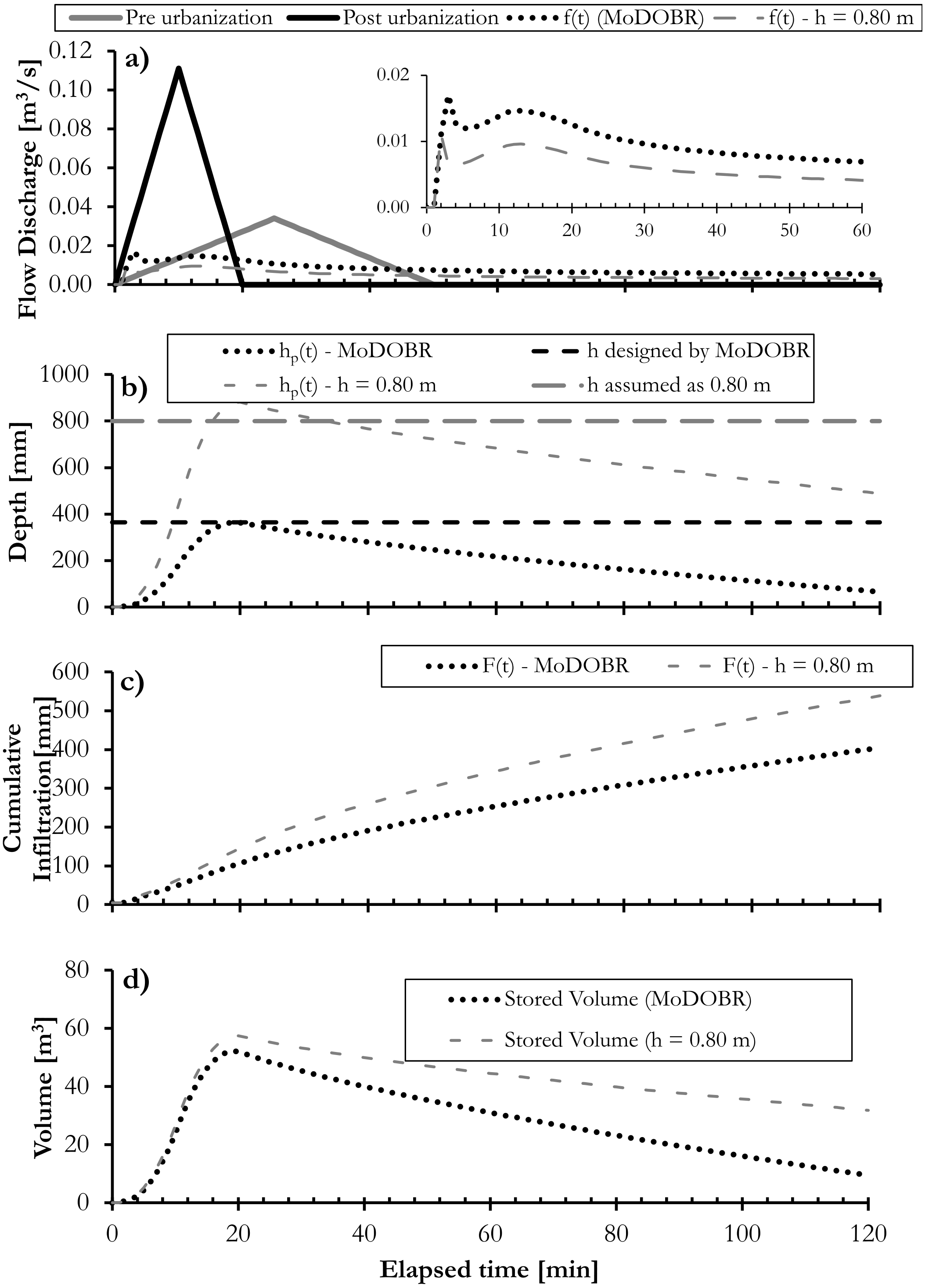

Figure 2: Simulation results comparing an arbitrary height of 0.80 m with the height calculated by Eq. (11). The temporal evolution of infiltration compared with the pre- and post-urbanization flows is presented in part (a). The ponding depth for the tested cases, compared with the design height h is presented in part (b). The accumulated infiltration of both cases is illustrated in part (c) and the temporal variation of the stored volume is shown in part (d).

Soil Type	k [mm · h^{-1}]	$\Delta\theta$	ψ [mm]
Sandy Loam	120.4	0.42	49.5
Loamy Sand	30.0	0.40	61.2
Sandy Clay	10.9	0.41	110.0
Clay	3.3	0.43	88.9
Silty Clay	6.6	0.49	166.9

Table 1: Parameters adopted for the simulation of different soil types, adapted from (Rossman and Huber, 2016).

4. Example 2 - Effect of different soil types for the same project

For the same data as in the previous problem, evaluate the effects of different soil types presented in Tab. 1 if the height were to be set at 0.8 m for reasons of technical feasibility. Then, calculate the compatible heights from Eq. (11) and check which soil types would meet the design conditions.

4.1. Solution

The results of the hydrological simulation for the various types of soil tested are presented in Fig. 3 and are the result of solving the problem for a simulation duration of $t_f = 1440$ min. It can be seen that only the Sandy and Clayey Sand soil types can release the stored ponding depth in less than 1440 min. However, the maximum ponding depths in both cases are 0.88 m and 0.95 m, both greater than the adopted design height of 0.8 m.

As mentioned previously, only sandy soil and clayey sand were able to guarantee detention times less than or equal to 1 day for the case of the height simply adopted as 0.8 m, as illustrated in Fig. 3(b). However, if the heights are compatible, all design solutions solving the problem of Eq. (11) result in emptying times less than 1 day for all soils, as illustrated in Fig. 4, being theoretically viable solutions. The results of the calculation of the compatible height and the percentage of the basin that should be composed of the LID to be able to store the excess volume and not overflow are presented in Fig. 5.

5. Example 3 - Use of drains in cases where area and height have limitations

Returning to calculation example 1 where the height was adopted as 0.80 m, it can be seen that the ponding depth was higher than the projected 0.80 m, generating an incompatible design. Solving Eq. (11) for this case, results in a height of 36 cm, but an area of 143 m^2. Assuming that there is a design restriction for the height to be 0.80 m, the area must therefore be 65.18 m^2, as shown in example 1. To guarantee the area required for the height of 0.80 m, design a drainage system in perforated underdrains so that the flooded height, for the design condition, is 0.80 m, which guarantees the volume required by the zero impact criterion.

The orifices can be modeled by (Porto, 2004):

$$S(t) = n_o \cdot C_d \cdot A_{\text{ef}} \sqrt{2g \cdot (\max{(h_p(t) - h_0), 0)}}$$

where $A_{\text{ef}} = \pi D^2/4$ is the effective area of the orifice, D is the diameter of the orifice, g is the acceleration of gravity, and h_o and n_o are the number of orifices.

Determine the number of underdrains n_o, for an adopted diameter of 25.4 mm, in order to guarantee the ponding depth of 88 cm lowered to the adopted height of 80 cm. Also determine the effective width of the spillway, assuming a coefficient of climatic changes (γ) of 1.2.

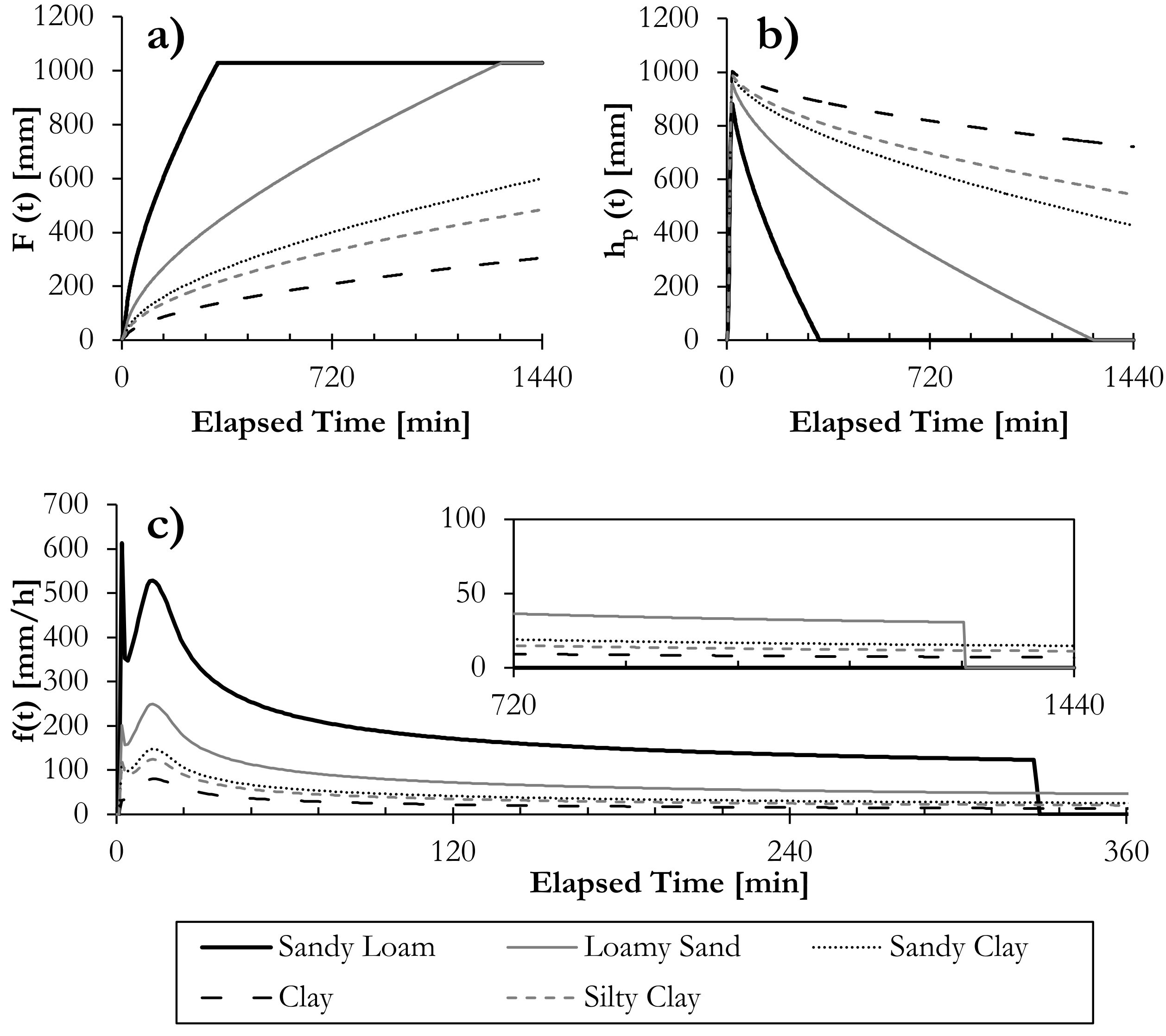

Figure 3: Simulation results for a height h of 0.8 m and for the different soil types presented in Tab. 1 for the design of a detention basin with a volume of 52.14 m^3. Part (a) represents the accumulated infiltration, (b) the ponding depth and (c) the infiltration rate, modeled by Eq. (7).

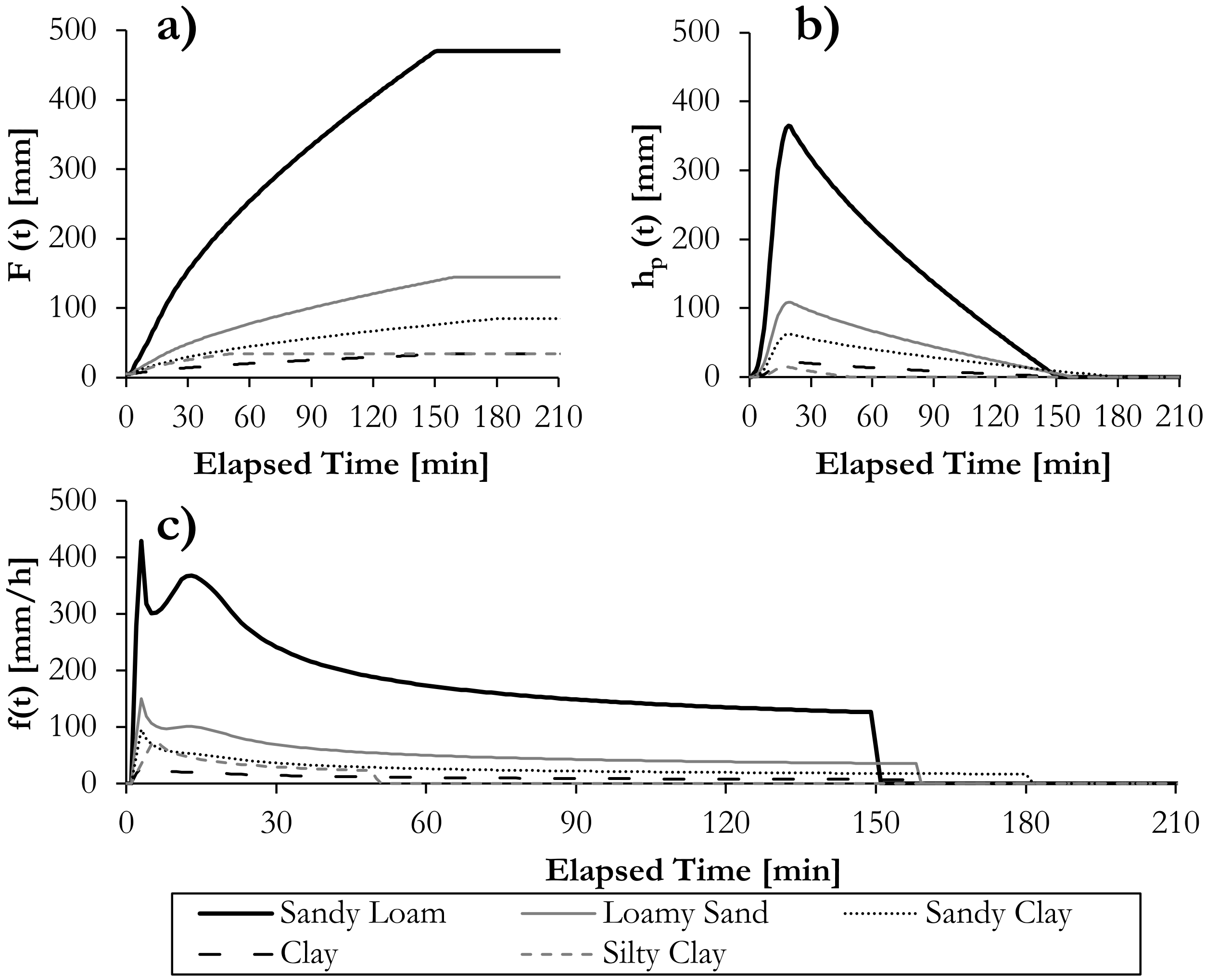

Figure 4: Simulation results for a height h optimized by Eq. (11), for the different types of soils presented in Tab. 1 for the design of a detention basin with a volume of 52.14 m^3. Part (a) represents the accumulated infiltration, (b) the ponding depth and (c) the infiltration rate, modeled by Eq. (7).

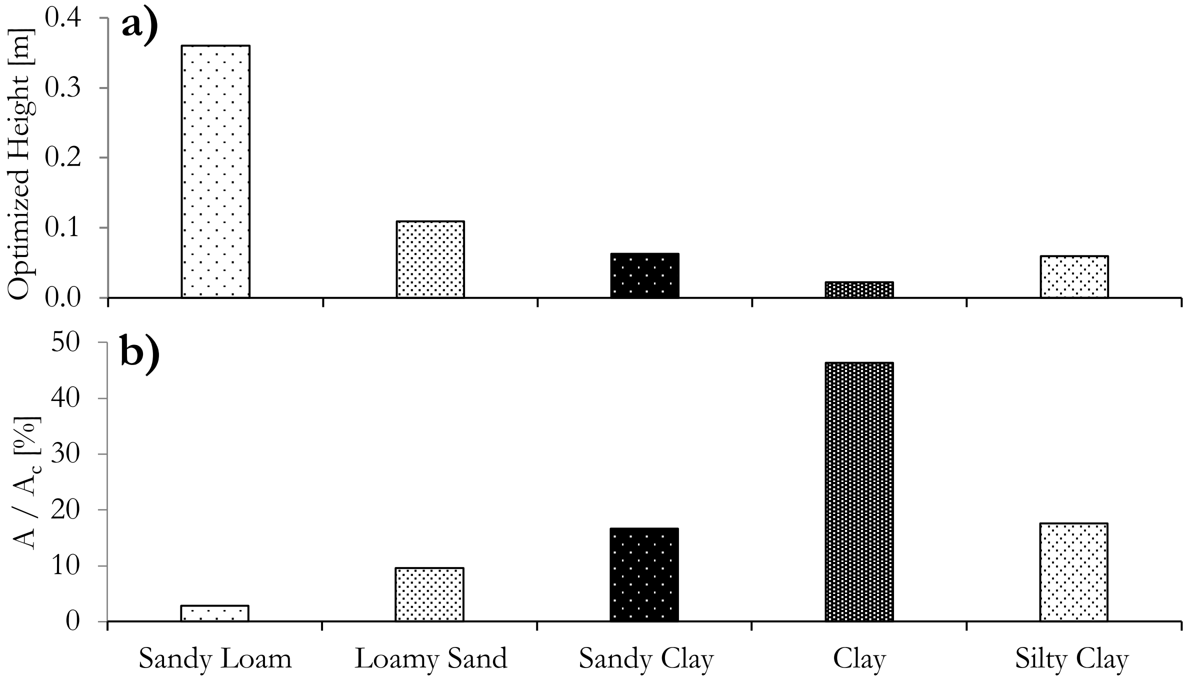

Figure 5: Heights compatible to avoid overflow and guarantee the minimum volume (a) and percentage of the basin that should be made available for the construction of the detention basin (b). A is the area of the retention basin and A_c is the drainage area of the contribution basin.

5.1. Solution

It is necessary to include the source term $S(t)$ in the model, specifically in Eq. (9). Adopting a diameter of 25.4 mm, the problem consists of evaluating, by trial and error, the number of 25.4 mm perforated drains that result in a height of 80 cm. The results of the evolution of the ponding depths for 0, 2, 4, 6 and 7 bottom holes with a diameter of 25.4 mm are presented in Fig. 6. In all cases, the surface area is constant.

It can be seen that 7 perforated drains with a diameter of 25.4 mm are capable of reducing the maximum ponding depth to the specified 80 cm. A greater number of underdrains favors faster drainage, which increases the excess peak flows and reduces emptying times. Thus, increasing the number of drains too much can decrease the reduction in peak flow and accelerate peak times.

The freeboard calculated by Eq. (13) as:

$$h_b = \frac{C_{\text{pos}} \cdot \Big[(\gamma - 1) \cdot i(\text{TR})\Big] \cdot A_c \cdot t_c}{A} = \frac{0.76 \cdot \Big[(1.2 - 1) \cdot 105.2\Big] \cdot 5000 \cdot 10 \cdot 60}{65.18} = 0.20 \text{ m}$$

The surface spillway calculation is made for a return period of 10 years, greater than that of the retention basin design, which is 5 years. Solving Eq. (14), we obtain:

$$L_{\text{ef}} = \frac{C_{\text{pos}} \cdot i_d(10) \cdot A}{C_d \cdot (h + h_b - h_s)^{3/2}} = \frac{0.76 \cdot 115.76 \cdot 1.20 \cdot 5000}{1.6 \cdot (0.8 + 0.2 - 0.8)^{3/2}} = 100 \text{ cm} \tag{16}$$

6. Local Sensitivity Analysis of Parameters

Taking into account the peak infiltration flow rate, the maximum ponding depth and the emptying time, a sensitivity analysis of the soil parameters that represent the hydrological properties of the filter medium is performed. This analysis is performed for the soil type in Tab. 1. Six intervals of percentage variation

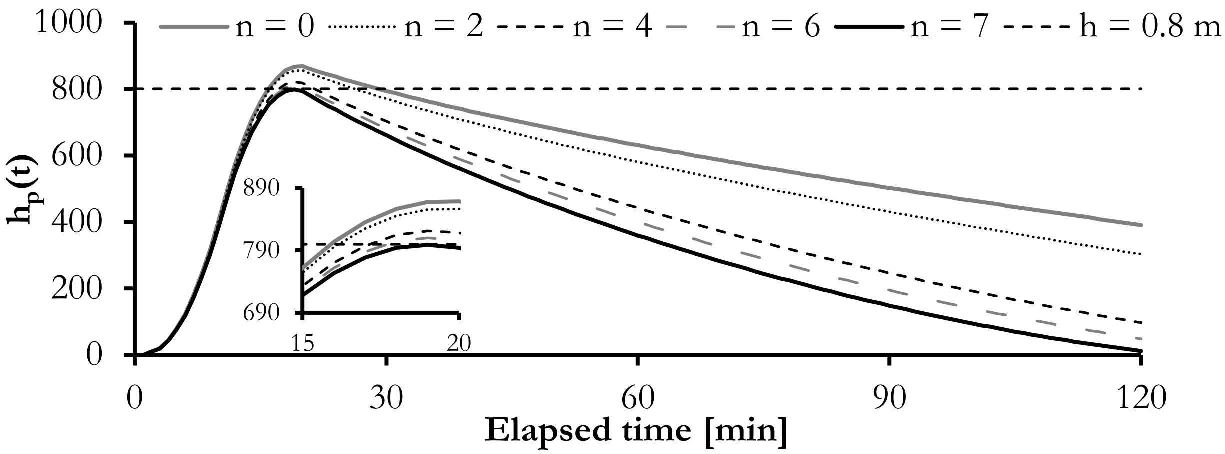

Figure 6: Influence of the number of orifices adopted. In this analysis, the discharge coefficient was adopted as 0.6 and n indicates the number of orifices. The dashed black line indicates the design height.

from a base value are taken into account, ranging from -75%, -50%, -25%, 0%, 25%, 50% and 75% in the parameters and computing the relative percentage deviations of the output functions. The base scenario for this analysis is calculation example 1, where a 5-year return period rainfall is simulated in a basin with an area of 5,000 m^2 and an average runoff coefficient of 0.76.

The objective of this analysis is to evaluate the individual effect of each parameter on the model results and thus identify which parameters should be adopted with more caution in the design. The results of the local sensitivity analysis are presented in Fig. 7.

.

Of the infiltration parameters, saturated hydraulic conductivity and moisture deficit are the most sensitive to changes. However, a different scenario may be observed if the base parameters were those of a clayey soil.

7. Discussions

The results of Example 1 indicate that, for a given design soil, the arbitrary choice of height is not valid for the design of retention basins and can result in both undersizing or oversizing. For example, in the case of detention basins that do not have infiltration, however, to retain excess runoff, the specification of a height can be compensated with the area. The converse is not true for retention basins, since the arbitrary choice infers in the calculation of infiltration, which can generate solutions that would cause an overflow given the non-linearity of infiltration. The examples shown in this article take as a criterion the minimum dimensions required to store the volume of excess urbanization if the soil is clogged and if the drainage devices are not functioning.

Example 2 shows the sensitivity of different soil types to meet a minimum volume and fixed inlet hydrograph. Once again, the arbitrary choice of a design height resulted in poorly designed basins for all soils, including 3 of the 5 soil types that did not meet the maximum emptying time due to being poorly designed. In the two cases where the maximum emptying time was respected, the ponding depths were higher than the adopted height, indicating that an iterative problem is necessary to couple the heights. Especially in the case of clayey-silty and clayey soils, underdrains can help reduce the areas required to make the heights compatible. The results from the solution of the proposed sizing problem, however, enabled theoretically viable solutions for all types of soil, with maximum emptying times of approximately 2h30 for a 10-minute rainfall, as shown in Fig. 2. Especially in the case of soils with reduced hydraulic capacities (e.g., soil with a sandy clay or clay texture), areas of 20 to 50% of the contribution basin and heights lower than 10 cm were required. Sandier soils presented solutions with smaller required areas, 2.9 and 9.5%, respectively, and are possibly more attractive for designing retention basins without underdrains.

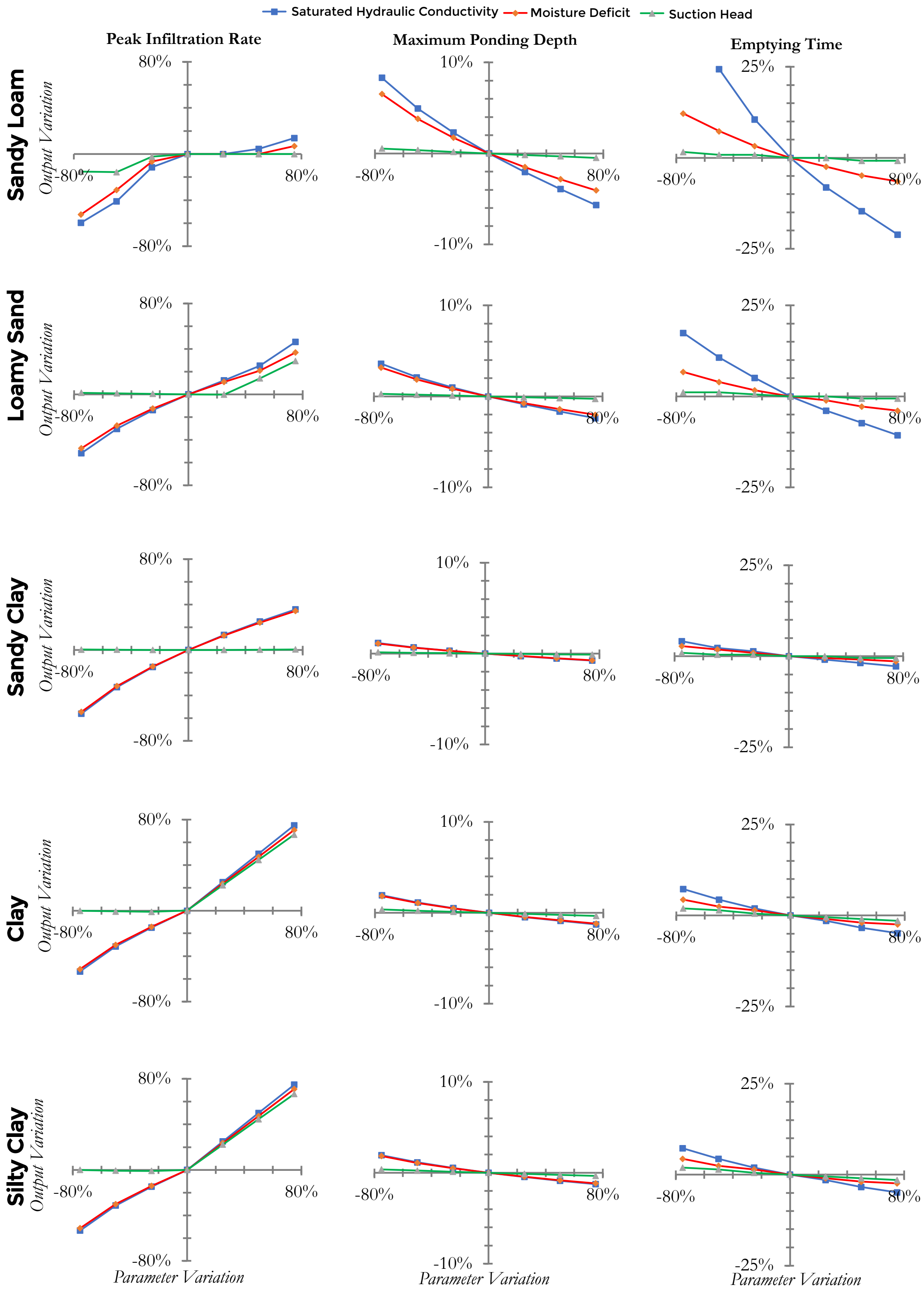

Figure 7: Results of the local sensitivity analysis for each of the soil types tested. Each row represents a soil type. The columns from left to right represent the sensitivity of the peak infiltration flow rate, ponding depth and emptying time, respectively, in relation to variations in saturated hydraulic conductivity, effective porosity and matric suction potential.

The effect of underdrains and freeboard design is presented in Example 3. In cases where the height is arbitrarily chosen, it is possible to ensure compatible heights and adequate detention times by correctly specifying the underdrain design. The results indicate, however, a high sensitivity of the ponding depth in relation to the diameter and number of holes. Since these are perforated drains and typically filled with filter material (e.g., gravel), the use of discharge coefficients between 0.3 and 0.6 is recommended.

The results of the sensitivity analysis for a typical design condition indicate that the saturated hydraulic conductivity k_{sat} is the most sensitive parameter for all metrics tested for all soil types. The effective porosity ($\Delta\theta$) has a similar effect, although slightly lower, than k_{sat}, both for peak discharge and ponding depth. However, the emptying time is about twice as sensitive to k_{sat} than to $\Delta\theta$. The effect of the matric suction potential is more significant in clayey-silty and clayey soils, and the impact of its increase is of the same importance as the increase in k_{sat} and $\Delta\theta$ in these cases. The results of this analysis allow the reader to identify the effect of uncertainties on the parameter estimates and also to evaluate the impact of aging and loss of efficiency of the LID, especially due to clogging of the porous medium that directly affects the effective porosity.

8. Conclusions

The Model for Optimized Sizing of Retention Basins (MoDOBR) was developed and applied in four numerical examples. The model is relatively easy to apply and can be solved in electronic spreadsheets. An open-source tool was developed and available to replicate all results and design infiltration techniques. The model requires basic data from the catchment and physical properties of the soil at the base of the retention basin. The methods presented in this text can be adapted to other infiltration techniques such as rain gardens, retention basins, detention basins (assuming null infiltration) and permeable pavements.

The results of calculation examples 1, 2, 3 and the sensitivity analysis support the following conclusions:

- The incompatibility of the design height of the retention basin with the maximum flooded height can lead to both undersizing or oversizing. If it is necessary to adjust the height or the design area due to a site specific constraint, the use of perforated underdrains can be a solution to make the heights compatible.
- There is only one compatible height and the proposed problem has a unique solution, given the minimum and maximum height constraints that are comprehensive enough to cover the solution space. This technique allows the use of solvers based on gradient algorithms to solve the problem. In the case of Excel, the nonlinear GRG solver is a fast-converging algorithm that is easy to use and applicable to the problem proposed in this article.
- The proposed method is such that, in the event of complete soil clogging, the available volume on the surface is capable of supporting the excess runoff generated by urbanization.
- The method for design the freeboard and surface spillway taking into account the effects of climate change is simple and easy to apply and requires only a coefficient that represents the increase in design intensity due to climate change. According to recent studies, this coefficient is in the order of 1.2 to 1.4.
- Saturated hydraulic conductivity is the most sensitive parameter, followed by effective porosity and matric suction potential. However, in predominantly clayey soils, the three parameters have approximately the same effects. In predominantly sandy soils, the effect of the matric potential is reduced.

Although the hydrograph tested in this text was the triangular hydrograph of the rational method, the model developed is applicable to any input hydrograph condition. A rainfall with duration equals the catchment time of concentration was assumed in this paper, though future research can investigate the effect of this approach for longer durations. Future work may incorporate lost opportunity costs due to land use, excavation costs, and labor costs in order to define a cost function that can be minimized, placing the compatibility of heights as a constraint in the optimization problem. The spreadsheet used to prepare the calculations in this article is freely available in an online repository accessible at (Gomes Jr., 2024).

References

M. B. Baptista, N. de Oliveira Nascimento, S. Barraud, Técnicas compensatórias em drenagem urbana, ABRH, 2011.

T. D. Fletcher, W. Shuster, W. F. Hunt, R. Ashley, D. Butler, S. Arthur, S. Trowsdale, S. Barraud, A. Semadeni-Davies, J.-L. Bertrand-Krajewski, et al., Suds, lid, bmps, wsud and more–the evolution and application of terminology surrounding urban drainage, Urban water journal 12 (2015) 525–542.

R. J. Winston, J. D. Dorsey, W. F. Hunt, Quantifying volume reduction and peak flow mitigation for three bioretention cells in clay soils in northeast ohio, Science of the Total Environment 553 (2016) 83–95.

E. R. d. C. Mano, et al., Estudo de bacias de retenção: como solução para situações crescentes de urbanização (2008).

C. Zoppou, Reverse routing of flood hydrographs using level pool routing, Journal of hydrologic engineering 4 (1999) 184–188.

M. N. G. Júnior, Aspectos hidrológicos-hidráulicos e avaliação da eficiência de biorretenções: modelos, princípios e critérios de projeto de técnicas compensatórias de 3ª geração, Ph.D. thesis, Universidade de São Paulo, 2019.

M. N. Gomes Jr, M. H. Giacomoni, M. B. de Macedo, C. A. F. do Lago, J. A. T. Brasil, T. R. P. de Oliveira, E. M. Mendiondo, A modeling framework for bioretention analysis: Assessing the hydrologic performance under system uncertainty, Journal of Hydrologic Engineering 28 (2023) 04023025.

L. T. L. M. Ferreira, M. G. F. P. d. Neves, V. C. B. d. Souza, Puls method for events simulation in a lot scale bioretention device, RBRH 24 (2019) e36.

L. A. Rossman, W. C. Huber, Storm water management model reference manual volume iii—water quality, US EPA National Risk Management Research Laboratory: Cincinnati, OH, USA (2016).

R. W. Skaggs, M. Youssef, G. Chescheir, Drainmod: Model use, calibration, and validation, Transactions of the ASABE 55 (2012) 1509–1522.

A. S. Braswell, R. J. Winston, J. D. Dorsey, M. A. Youssef, W. F. Hunt, Calibration and validation of drainmod to predict long-term permeable pavement hydrology, Journal of Hydrology (2024) 131373.

PG County, Bioretention manual, Prince George's County, Maryland, Department of Environmental Resources, Environmental Services Division, Landover, MD (2007).

A. Rosa, Bioretention for diffuse pollution control in SUDS using experimental-adaptive approaches of ecohydrology, Ph.D. thesis, Universidade de São Paulo, 2016.

D. M. Santos, J. A. Goldenfum, F. Dornelles, Outflow adjustment coefficient for the design of storage facilities using the rain envelope method applied to brazilian state capitals, Revista Ambiente & Água 16 (2021) e2707.

A. d. Silveira, J. A. Goldenfum, Metodologia generalizada para pré-dimensionamento de dispositivos de controle pluvial na fonte, Revista Brasileira de Recursos Hídricos 12 (2007) 157–168.

P. Tomaz, Aproveitamento de água de chuva, São Paulo: Navegar (2003) 355–359.

L. D. Duke, M. N. Mullen, K. E. Unger, R. Rotz, S. Thomas, Flood mitigation: Regulatory and hydrologic effectiveness of multicomponent runoff detention at a southwest florida site, JAWRA Journal of the American Water Resources Association 60 (2024) 189–210.

L. A. Richards, Capillary conduction of liquids through porous mediums, Physics 1 (1931) 318–333.

W. H. Green, G. Ampt, Studies on soil phyics., The Journal of Agricultural Science 4 (1911) 1–24.

R. Paiva, W. Collischonn, P. Miranda, I. Petry, F. Dornelles, J. Goldenfum, F. Fan, A. Ruhoff, H. Fagundes, Critérios hidrológicos para adaptação à mudança climática: Chuvas e cheias extremas na região sul do brasil, Instituto de Pesquisas Hidráulicas (2024).

T. J. Mulvaney, On the use of self-registering rain and flood gauges in making observations of the relations of rainfall and flood discharges in a given catchment, Proceedings of the Institution of Civil Engineers of Ireland 4 (1851) 18–33.

E. Kuichling, The relation between the rainfall and the discharge of sewers in populous districts, Transactions of the American Society of Civil Engineers 20 (1889) 1–56.

A. L. L. d. Silveira, Desempenho de fórmulas de tempo de concentração em bacias urbanas e rurais, Rbrh: revista brasileira de recursos hídricos. Porto Alegre, RS: ABRH. Vol. 10, n. 1 (jan./mar. 2005), p. 5-23 (2005).

NRCS, Part 630 National Engineering Handbook, Chapter 15: Time of Concentration, (210–vi–neh, may 2010 ed., Natural Resources Conservation Service, 2010.

M. Gomes Jr, P. Braga, E. Mendiondo, L. Reis, Statistical, visual and non-parametric analises for tuning optimization of idf curves and construction of abacuses for hydraulic projects: Case study in Sao Carlos - SP, Revista DAE 69 (2021).

M. N. Gomes Júnior, M. H. Giacomoni, A. F. Taha, E. M. Mendiondo, Flood risk mitigation and valve control in stormwater systems: State-space modeling, control algorithms, and case studies, Journal of Water Resources Planning and Management 148 (2022) 04022067.

J. G. Lee, M. Borst, R. A. Brown, L. Rossman, M. A. Simon, Modeling the hydrologic processes of a permeable pavement system, Journal of Hydrologic Engineering 20 (2015) 04014070.

S. Smith, L. Lasdon, Solving large sparse nonlinear programs using grg, ORSA Journal on Computing 4 (1992) 2–15.

R. d. M. Porto, Hidráulica básica (2004).

Gomes Jr., Modelo de dimensionamento otimizado de bacias de retenção, https://github.com/marcusnobrega-eng/MoDOBR, 2024.